NUMERICAL INVESTIGATION OF OPERATING PRESSURE EFFECTS ON THE PERFORMANCE OF A VORTEX TUBE

by

Nader POURMAHMOUD [a*], ***Amir HASSANZADEH*** [b], ***and Omid MOUTABY*** [a]

[a] Department of Mechanical Engineering, Urmia University, Urmia, Iran
[b] Department of Mechanical Engineering, College of Engineering, Mahabad Branch, Islamic Azad University, Mahabad, Iran

Original scientific paper
DOI: 10.2298/TSCI110907030P

A three-dimensional computational fluid dynamics simulation of a vortex tube has been carried out to realize the effects of operating pressure. The highly rotating flow field structure and its characteristic are simulated and analyzed with respect to various operating inlet pressure ranges. Numerical results of compressible and turbulent flows are derived by using of the standard k-ε turbulence model, where throughout the vortex tube was taken as a computational domain. The main object of the present research is to focus on the importance of identifying the suitable inlet gas pressure corresponds to used vortex tube geometry. Achieving a highly swirling flow and consequently maximum cold temperature difference were the key parameters of judgment. The results revealed that these acceptable conditions of machine performance can be provided when the inlet operating pressure is appropriate both to mechanical structure of machine and physical properties of working fluid. The stagnation point location in the axial distance of vortex tube and Mach number contours in the vortex chamber as additional information are extracted from flow filed; such that interpretation of shock wave formation regions may be accounted as significant features of investigation. Finally, some results of the computational fluid dynamics models are validated by the available experimental data and shown reasonable agreement, and other ones are compared qualitatively.

Key words: *vortex tube, numerical simulation, operating inlet pressure, energy separation, mach number*

Introduction

Vortex tube or Ranque-Hilsch vortex tube is a mechanical device with a simple geometry, which is able to split the entrance tangential compressed gas into different hot and cold streams. In this way, the inlet high pressure gas enters the vortex chamber tangentially through one or more nozzles, and then energy separation mechanism occurs. This machine does not have any moving parts, and merely operates due to entrance of a working fluid; that is arbitrary taken as compressed air. Separated cold or hot streams, can be employed according to the industrial requirements. However, the noticeable function of a vortex tube is almost spot cooling process.

* Corresponding author; e-mail: n.pormahmod@urmia.ac.ir

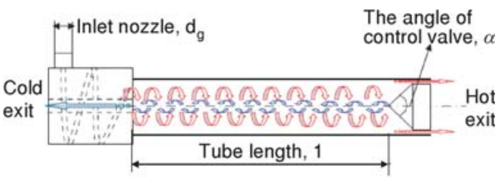

Figure 1. Schematic drawing of a vortex tube and its components [21]

This device was invented many years ago, when the first time it was discovered accidentally by George Ranque a French physicist in 1931 [1], while he was conducting a research over vortex tube in the field of dust separation. He noticed the emitting of hot air from onside and cold air from another side.

A few years later, in 1945 Rudolf Hilsch German physicist worked on vortex tube consequently. He developed the vortex tube principles, and worked on its designing parameters. He finally published the results of his works in an article in 1947 [2]. In fig. 1 a vortex tube and its components is schematically displayed. In the recent years, the techniques of computational fluid dynamics (CFD) modeling have been developed for more survey and clarification. After them, Elser and Hoch [3], Martynovskii and Alekseev [4], Takahama [5], Bruun [6], and Skye *et al.* [7], carried out important experimental investigations on the vortex tube. Fulton [8] presented analytical analysis on energy separation, velocity and temperature profiles in vortex tube. Deissler and Perlmutter [9], Young and Mc Cutcheon [10], Ahlborn *et al*. [11], and Stephan *et al.* [12, 13] investigated energy separation analytically in this system. Dincer *et al.* [14], Kirmaci [15], Akhesmeh *et al.* [16], Bramo and Pourmahmoud [17-19] and Pourmahmoud *et al.* [20] investigated effective parameters influence on the vortex tube performance. In spite of existing extensively research sources about vortex tube, understanding of its energy separation mechanism know-how needs some thinkable investigations yet.

Some experimental and numerical studies have been conducted to realize the effect of inlet operating pressure of a vortex tube. Stephan *et al*. [13], both analytically and experimentally investigated the influence of this parameter for various kind of gases such as air, helium and oxygen. At their study, the inlet pressure was adjusted in the range of 1.5 to 5 bar for air, 1.5 to 4 bar for oxygen, and 1.5 to 3 bar for helium. They concluded that cold exit temperature difference increases due to increase of inlet pressure. Dincer *et al.* [14] performed an experimental investigation about the effects of length to diameter ratio and nozzle number on the performance of vortex tubes for different inlet pressure from 200 to 320 kPa. They invoked similar conclusion to Stephan *et al.* [13]. Aydin and Baki [21] studied the thermal performance as a function of the following geometrical parameters under different inlet pressures: length of the vortex tube, diameter of the inlet nozzle, and angle of the control valve.

In the tested pressure ranges of 3, 4, and 5 bar, they inferred that higher inlet pressure causes to greater temperature difference of the outlet streams. Kirmaci and Uluer [22] discussed the results of an experimental investigation of a vortex tube performance that was related cold mass fraction, inlet pressure, and nozzles number to each other. The experiments of performance analyzing were carried out upon 150-700 kPa operating pressure with 50 kPa increments. They concluded that under higher operating pressure conditions, high cold mass fraction gives greater air flow, but it does not possibly give the lowest temperatures.

It can be deduced that, these researchers have believed to an appropriate inlet pressure which can produce reasonable performance for a vortex tube. Perhaps, if their experimental tests were continued, they would obtain the proper operating pressure value for each of tested devices. Although all of the mentioned articles shown that thermal energy separation increases by increase of P_{in}, energy consumption of operated vortex tube grows very rapidly. So far, there are not seen comprehensive CFD researches on the influence of inlet gas pressure on the performance of a vortex tube. However, as a common point, available numerical data imply to increase of cold and hot exit temperature difference due to increase of inlet pressure.

Ameri and Behnia [23] showed that if the inlet pressure increases up to a certain value, the efficiency of vortex tube will increase. Nevertheless, operating pressure increasing greater than their reported value yields decreasing of efficiency. Their numerical simulation were conducted for inlet pressure range of 6 bar, so that pressure inlet 5 bar was taken as critical operating condition. At the higher pressures than 5 bar, any increasing in the inlet pressure leads to a significant decrease of efficiency. The same type of results was reported by Zhidkov *et al.* [24], who that concluded $\Delta T_{\mathrm{i,c}}$ increases by increasing of inlet pressure only in a particular operating pressure domain.

In this way, the present research has believed that any vortex tube with a defined geometry should be operated in a definite operating inlet pressure to attain reasonable performance. Although, general expectation for actuating of a vortex tube with any inlet pressure whether low or high would be acceptable, its cooling criteria (cold temperature difference) would not be economical from engineering point of view. Obviously, the vortex tube thermo dynamical efficiency is not justifiable, however it would be logical to capture both economical consideration and attaining to an inlet pressure ranges causing maximum cold temperature difference.

Numerical modeling and governing equations

The flow field through vortex tube has been modeled by using of the FLUENT$^{\mathrm{TM}}$ software package. These CFD models explore a three dimensional, steady-state, compressible, and turbulent flow. Literature survey has shown that the standard *k*-*ε* turbulence model can satisfy description of complex flow behavior in the vortex tube [18]. In addition, compressible and turbulent flow in the vortex tube are governed by well-known mass, momentum and energy conservation equations as:

$$\frac{\partial}{\partial x_j}(\rho u_j) = 0 \tag{1}$$

$$\frac{\partial}{\partial x_j}(\rho u_i u_j) = -\frac{\partial p}{\partial x_i} + \frac{\partial}{\partial x_j}\left[\mu\left(\frac{\partial u_i}{\partial x_j} + \frac{\partial u_j}{\partial x_i} - \frac{2}{3}\delta_{ij}\frac{\partial u_k}{\partial x_k}\right)\right] + \frac{\partial}{\partial x_j}(-\overline{\rho u_i' u_j'}) \tag{2}$$

$$\frac{\partial}{\partial x_i}\left[u_i\rho\left(h + \frac{1}{2}u_j u_j\right)\right] = \frac{\partial}{\partial x_i}\left[k_{\mathrm{eff}}\frac{\partial T}{\partial x_j} + u_i(\tau_{ij})_{\mathrm{eff}}\right], \quad k_{\mathrm{eff}} = K + \frac{c_p \mu_{\mathrm{t}}}{\mathrm{Pr_t}} \tag{3}$$

Additional equation, because of compressibility effect is state equation:

$$p = \rho RT \tag{4}$$

The standard *k*-*ε* turbulence model imposes the turbulence kinetic energy, *k*, and its rate of dissipation, *ε*, equations as can be written:

$$\frac{\partial}{\partial \mathrm{t}}(\rho k) + \frac{\partial}{\partial x_i}(\rho k u_i) = \frac{\partial}{\partial x_j}\left[\left(\mu + \frac{\mu_{\mathrm{t}}}{\sigma_{\mathrm{k}}}\right)\frac{\partial k}{\partial x_j}\right] + G_{\mathrm{k}} + G_{\mathrm{b}} - \rho\varepsilon - Y_{\mathrm{M}} \tag{5}$$

$$\frac{\partial}{\partial \mathrm{t}}(\rho k) + \frac{\partial}{\partial x_i}(\rho k u_i) = \frac{\partial}{\partial x_j}\left[\left(\mu + \frac{\mu_{\mathrm{t}}}{\sigma_{\varepsilon}}\right)\frac{\partial \varepsilon}{\partial x_j}\right] + C_{1\varepsilon}\frac{\varepsilon}{k}(G_{\mathrm{k}} + C_{3\varepsilon}G_{\mathrm{b}}) - C_{2\varepsilon}\rho\frac{\varepsilon^2}{k} \tag{6}$$

where G_k represents the generation of turbulence kinetic energy because of the mean velocity gradients and G_b – the generation of turbulence kinetic energy due to buoyancy, which is neglected in this case. Y_M represents the contribution of the fluctuating in compressible turbulence to the overall dissipation rate and $C_{1\varepsilon}$, $C_{2\varepsilon}$, and $C_{3\varepsilon}$, are coefficients. σ_k and σ_ε are the turbulent Prandtl numbers for k and ε, respectively. The turbulent viscosity, μ_t, is computed by combining k and ε such that:

$$\mu_t = \rho C_\mu \frac{k^2}{\varepsilon} \tag{7}$$

where C_μ is kept a constant value, and the model constants $C_{1\varepsilon}$, $C_{2\varepsilon}$, C_μ, σ_k, and σ_ε have the following default values of: $C_{1\varepsilon} = 1.44$, $C_{2e} = 1.92$, $C_\mu = 0.09$, $\sigma_k = 1.0$, and $\sigma_\varepsilon = 1.3$.

Physical modeling

Figure 2 represents the computational domain for the studied vortex tube. The present CFD model is established based on the model which was introduced by Skye *et al*. [7]. It is noteworthy that, an Exair^{TM} 708 slpm vortex tube was used by Skye to collect all of the experimental data. The geometrical details of this vortex tube are given in tab. 1. The mentioned Skye's vortex tube utilizes six numbers of straight nozzles. Thus, this type of vortex tube has a vortex chamber with radius of 5.7 mm, and the nozzles are located tangentially to it. Since the computational domain has an axisymetry, then the CFD model has been assumed a rotational periodic condition. Hence, only a sector of the flow domain with angle of 60° needs to consider for computations as shown in fig. 2(b).

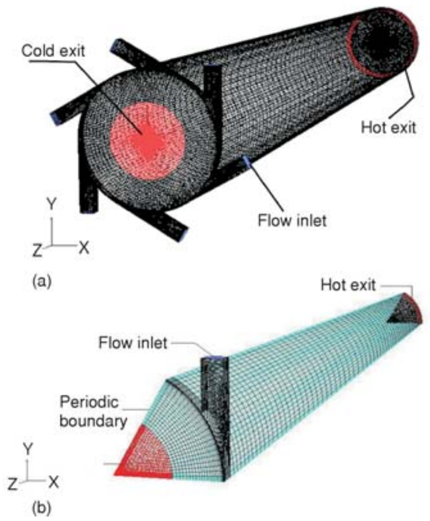

Figure 2. (a) 3-D model of vortex tube, (b) a sector of computational domain

Table 1. Geometrical details of Skye's vortex tube

Measurement	Value
Working tube length	106 mm
Vortex tube diameter	11.4 mm
Nozzle height	0.97 mm
Nozzle width	1.41 mm
Nozzle total inlet area (A_n)	8.2 mm^2
Cold exit diameter	6.2 mm
Cold exit area	30.3 mm^2
Hot exit diameter	11 mm
Hot exit area	95 mm^2

In deriving of numerical results, the created CFD model is to be subjected to various ranges of mass flow rate ($\dot{m}_{in}$), and inlet pressure (P_{in}). These successively numerical analyses have been accomplished until providing a reasonable operating pressure.

Boundary conditions of analysis

Flow boundary conditions for the CFD model were determined based on Skye's experimental measurements. Therefore, the inlet is modeled as a mass flow inlet equal to 8.35 gs^{-1}, and stagnation temperature 294.2 K, respectively. The static pressure at the cold exit boundary is fixed to experimental measurements pressure that is 0.15 bar, and for the hot exit boundary it must be adjusted corresponds to desired cold mass fraction. In addition, a no-slip velocity boundary condition is enforced on all of the walls of vortex tube, and simultaneously they are assumed to be adiabatic. Figure 3 shows the reversed flow at cold exit, since the CFD model predicts that reversed flow will occur at the cold exit at low cold gas fractions, and then the backflow temperature value is set to 290 K.

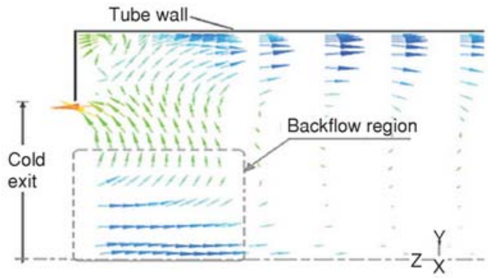

Figure 3. Reversed flow through cold exit at low cold gas fraction

Another boundary condition which can be applied for hot outlet would be extending the outlet region and immediate modeling of ambient effect by pressure far-field boundary condition. Hence, in the present research a comparison have been performed for CFD models based on introduced different boundary conditions, namely pressure outlet and pressure far-field. In all of quantitative and qualitative comparisons, there are not seen any considerable differences; therefore, the pressure outlet boundary condition is utilized for both of hot and cold exit outlets. The comparative results are summarized in tab. 2. It should be mentioned that these results are obtained for special value of cold mass fraction α = 0.3.

Table 2. Comparison between pressure outlet and pressure far-field boundary conditions for hot outlet

Quantity	Pressure far-field	Pressure outlet	Difference [%]
T_c	250.85	250.24	0.243173
T_h	311.97	311.5	0.150656
$(Z/L)_v$	0.986	0.985	0.10142
T_{wmax}	10.714	310.119	0.191494
$(Z/L)_w$	0.834784	0.834784	0

Results and discussion

A CFD analysis has been carried out for an 11.4 mm diameter vortex tube with different inlet pressure to attain an appropriate operating pressure. In this way, several parameters such as cold exit temperature difference, maximum swirl velocity, stagnation point axial location, and occurring of shock wave in the vortex chamber are the main criteria of judgment in evaluation of operating pressure. Therefore, geometry of vortex tube is fixed and only the inlet pressure is altered until appearing of desired flow field behavior.

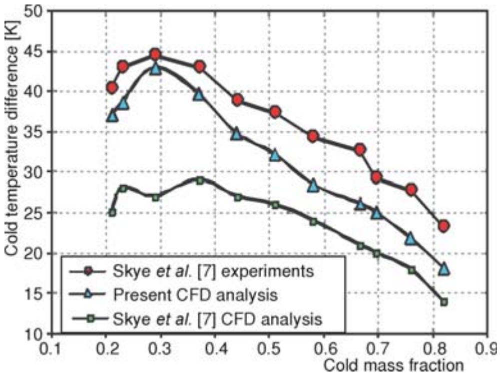

Figure 4. Comparison of cold exit temperature differences with the experimental data

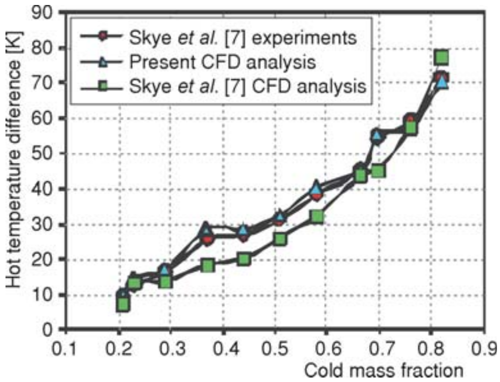

Figure 5. Comparison of hot exit temperature differences with the experimental data

Validation

The temperature separation obtained from the present numerical evaluations was compared with Skye's available experimental data and computational curves; which was developed in a 2-D form. Utilizing of the k-ε turbulence models in analyzing of a vortex tube complex flow field shown good results. Bramo and Pourmahmoud [18] showed that, because of good agreement of their numerical results with the experimental data, this model could be employed to simulate the effect of turbulence inside of vortex tube computational domain. Similarly, at the present research numerical simulations have been conducted for highly rotating and turbulent flow through the introduced vortex tube by this model.

As shown in figs. 4 and 5, the hot exit temperature difference $\Delta T_{h,i}$ predicted by the present CFD model is in good agreement with the experimental results. Prediction of the cold exit temperature difference $\Delta T_{i,c}$ is also found to be in lying between the experimental and computational results of Skye's.

Though both of models under predicted the cold exit temperature difference $\Delta T_{i,c}$, the predictions from the present study are found to be closer to the experimental results. The hot exit temperature differences $\Delta T_{h,i}$ are closer to experimental data in both present CFD simulation and Skye's calculations. The CFD model produces hot exit temperature of 363.2 K at 0.8 of cold mass fraction, and a minimum cold exit temperature of 250.24 K at about 0.3 cold mass fraction, respectively.

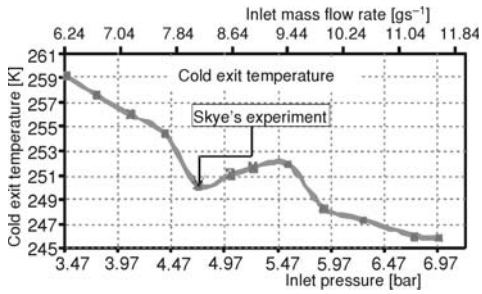

Figure 6. Cold exit temperature for different inlet pressure and mass flow rate, $\alpha = 0.3$

Effect of inlet pressure

In this section, the effect of inlet pressure (P_{in}) is studied such that an appropriate operating pressure is achieved. Figure 6 displays the changes of cold exit temperature *vs.* inlet pressure and correspondingly inlet mass flow rate ($\dot{m}_{in}$). Inlet pressure is changed from 3.47 to 7.24 bar, which is equal to mass flow rate of 6.24 to 12 g/s, respectively. The graph indicates that by increasing of inlet pressure from 3.47 to 4.8 bar (Skye's operating pressure), the cold exit temperature decreases. On the other hand, in the range of 4.8 to 5.71 bar, inlet pressure increasing gives rise to cold exit temperature. Continuation of inlet pressure increment from 5.71 bar, brings a drop of cold exit temperature again.

In the pressure range of 3.47 to 5.71 bar, the inlet pressure causing to approach a minimum cold exit temperature is 4.8 bar, which is equal to Skye's experimental value. This pressure provides a cold exit temperature equal to 250.24 K. Because of the importance of this data point, it is needed to maintain as a critical comparison value respect to the other data in the graph. At the mentioned operating pressure, the vortex tube uses a mass flow rate of 8.34 g/s.

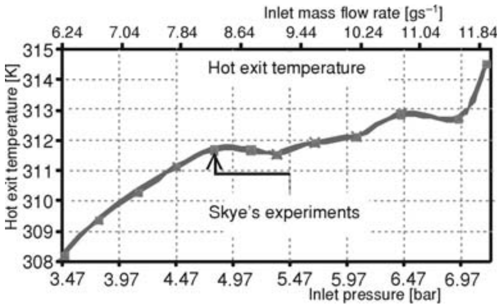

Figure 7. Hot exit temperature for different inlet pressure and mass flow inlet, α = 0.3

Figure 7 also shows the changes of hot exit temperature with respect to applied inlet pressure. Obviously, the overall behavior of diagram is increasingly, since the rotating gas flow is encounters by both shear stresses of layers and tube wall friction. Of course, it must be cited that in the pressure range of 5.13 to 7 bar, some negligible oscillations are seen in the trend of curve. Nevertheless, in summery hot exit temperature is continuously increased by increasing of inlet pressure.

A vortex tube is used most often for cooling, not for heating. Hence, cold temperature is more important. It is evident that the inlet pressure should be increased, whatever much more cooling we want. However, it requires more spending that is not economical. Therefore, the most optimized state to give low cold exit temperature and to be economical, in Skye's *et al*. experiment would be operating pressure equal to 4.8 bar. In that pressure, which is equivalent to mass flow rate of 8.34 g/s, the compressed air is injected to the system, and present CFD simulation confirms this condition again.

In fig. 8, the present numerical evaluations of pressure contours distribution are illustrated, according to Skye's test condition. Analyzing of pressure distribution in the vortex chamber helps to realize the flow field structure precisely.

Because of compressibility spirit of working fluid, this study would be better to couple with the formation of flow Mach number levels in the forgoing sections. An overall following of inlet pressure changes has revealed a continuous drop along of any nozzles, which is very negli-

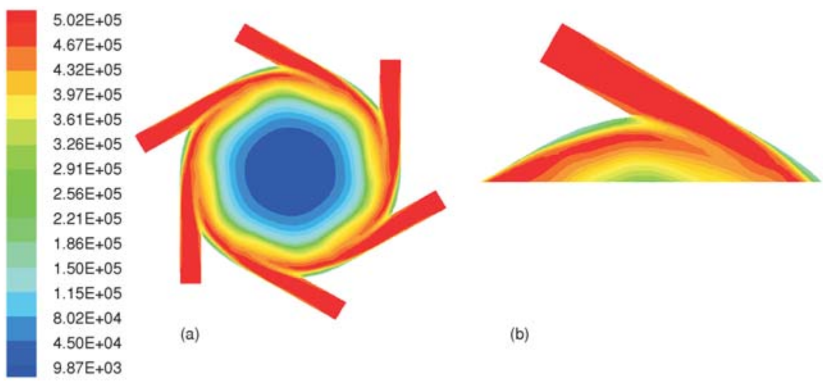

Figure 8.
(a) Pressure contours in the vortex chamber
(b) zoomed view at the nozzle exit end, α = 0.3
(for color image see journal web site)

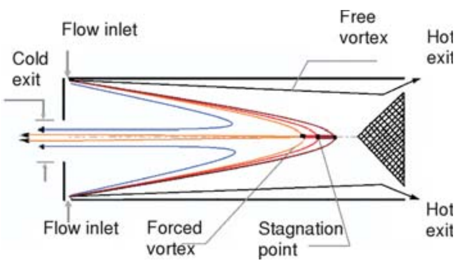

Figure 9. Schematically description of flow patterns through the vortex tube

gible in conducted CFD simulation. However, this compressible flow produced shock wave in the vortex chamber just after the nozzles exit end (in some of studied cases); so that the high pressure cores are formed in the chamber.

The effect of stagnation point location

The stagnation point position within the vortex tube can be determined based on velocity profile along the tube length at the point, where it ceases to a negative value. Figure 9 shows the stagnation point and corresponding streamlines in the r-z plane.

In the investigated models, positions of stagnation points are represented in fig. 10 that is a noticeable behavior. According to obtained results, the maximum amount of $Z/L = 0.9874$ is corresponds to operating pressure of 4.8 bar, which is closer to hot exit rather than other operating conditions. In spite of existing of a negligible difference between the different locations of stagnation point for various inlet pressures, these small values of difference make various cold exit temperatures accordingly.

However, the importance of actuating a vortex tube in a properly operating pressure is indicated in simultaneously comparing of both stagnation point location and cold exit temperature curves. Stagnation points locations curve are passing a normal procedure until Skye's experiment working pressure. Increasing of inlet pressure towards 5.71 bar completes maximum expectation of inlet pressure increasing. In contrast, raised inlet pressure beyond this value, makes an unbelievable behavior; since the axial locations of stagnation points are increased towards hot exit again. The objection to trend of this curve is due to conflict with the axial location of stagnation point as a criterion of good operating of any vortex tube. In addition, although those locations are taken toward hot exit respect to Skye's value; it doesn't cause significantly decreasing of cold exit temperature. From the numerical results of this graph it can be determined that Skye's operating pressure 4.8 bar is increased up to 50%, while cold exit temperature decreases only 4.21 K (1.68%).

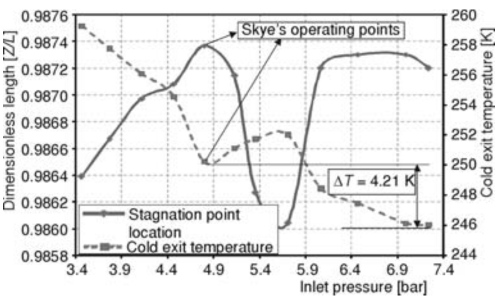

Figure 10. Locations of stagnation points for different inlet pressures, α = 0.3

Mach number investigation in the vortex chamber

Rarely studies have been implemented on the Mach number distribution in the vortex chamber. For example, Wu *et al* [25] designed a new nozzle with equal gradient of Mach number. Their device was equipped by a new intake flow passage of nozzles with equal flow velocity, and developed to reduce the flow loss. However, in the current study a considerable focus is devoted to this parameter of a compressible flow field. As shown in fig. 11, Mach number contours are distributed throughout the vortex chamber for inlet pressure 4.8 bar. It must be regarded that in the Skye's experiment for predicting of good operating condition (P_{in} = 4.8 bar), the present CFD analyses revealed Mach number levels with the maximum magnitude of 1.55 in the vortex chamber. Hence, it may be mentioned as evidence that Skye's experiment was not successful in higher inlet pressures to achieve lower values of cold exit temperature. Analyzing of compressible flow from inlet of any nozzles to location where it reaches to a highly rotating condition would be very important because of probability formation of strong and undesirable shock waves in the vortex chamber. This means that treating with the highly inlet pressure for a vortex tube should be regarded very consciously to avoid from occurring of shock wave and consequently energy losses. In other word, any irreversibility in the energy of flow in the vortex chamber implies to decrease of useful energy fraction that would be enhanced swirl velocity.

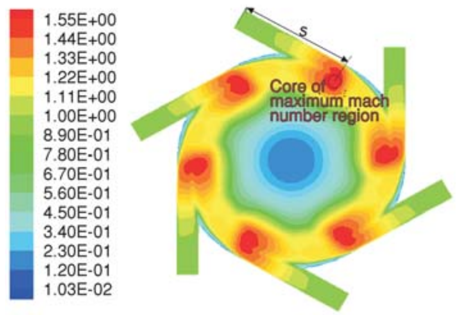

Figure 11. Mach number contours at the vortex chamber and schematically identifying of high Mach number region; P_{in} = 4.8 bar, α = 0.3 (for color image see journal web site)

According to fig. 11, that is a representation of flow field simulation with respect to Skye's operating pressure condition, the flow regime at the entrance of any nozzles is subsonic. Nevertheless, it reaches to higher values of Mach number about 0.7 to maximum 0.8. Through the nozzle channel, the range of Mach number remains approximately constant because of its short length, and finally at the entrance to vortex chamber it increases.

In the red colored region, Mach number level reaches to its maximum values, and then the fluid flow alters to a supersonic regime. Subsequently, because of occurring of a suddenly expansion process together with significant losses in flow layers, the Mach number drops to subsonic ranges. The formation of this complicated mechanism of energy losses might be related mainly to appearance of shock waves in exit domain of any nozzles, which are closer to next nozzle. The distance of nozzle entrance to core of high Mach number region is denoted by S. Successive evaluations shown that whatever inlet pressure increases both Mach number level and length of S increases; so that the core of this region goes far from the nozzle exit and moves towards the next nozzle.

Figure 12 represents almost a linear increase of maximum Mach number in the chamber, when inlet pressure given rise to 7.24 bar. Growing of length of S also obeys from increasing of inlet pressure and forms a semi linear curve (fig. 12).

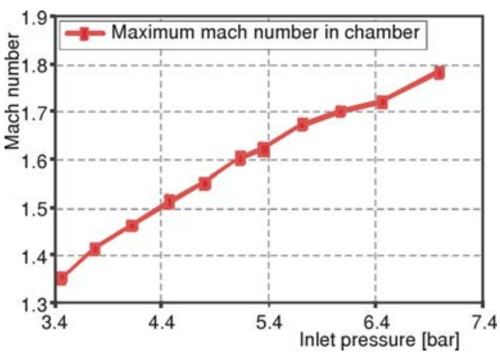

Figure 12. Maximum Mach number in the vortex chamber for different inlet pressures

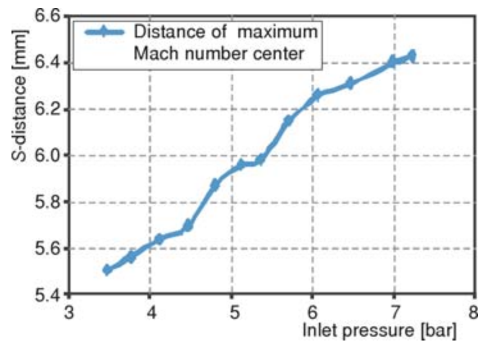

Figure 13. The distance between maximum Mach number core and inlet of nozzle for different inlet pressures

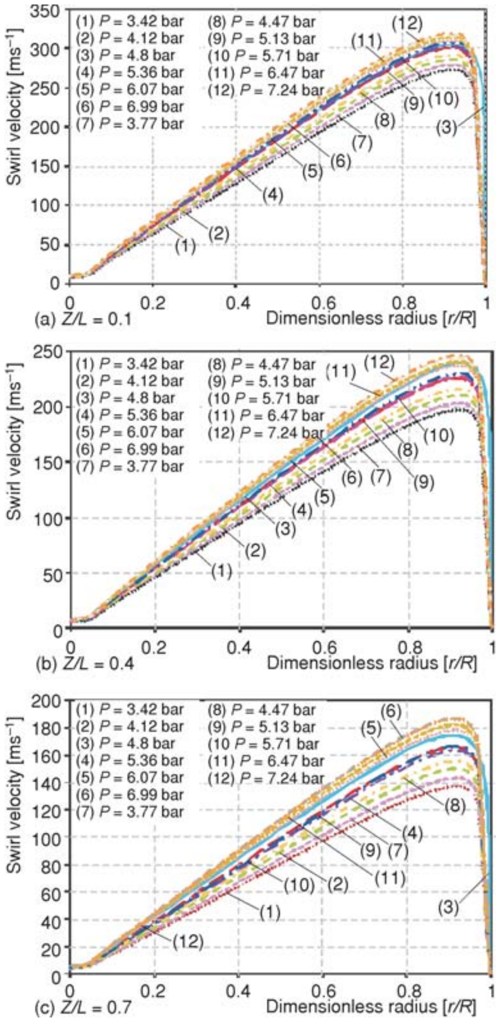

Figure 14. Radial profiles of swirl velocity at various axial location of tube; (a) *Z/L*= 0.1, (b) *Z/L*= 0.4, (c) *Z/L*= 0.7, α = 0.3
(for color image see journal web site)

Swirl velocity

Figure 14 illustrates the radial profiles for the swirl velocity at different axial locations of tube. The comparison of this criterion at the several axial locations proves its increase due to employ of higher inlet pressure. However, at the any inlet pressures, the magnitude of the swirl velocity decreases as ever moves towards the hot end exit. In spite of producing high swirl velocity because of applying larger values of inlet pressure, the valuable decreasing of cold exit temperate is not seen as discussed reasons in the previous sections. Numerical studies of swirl velocities have been revealed that axial location Z/L= 0.1 is one of the important locations in the neighborhoods of vortex chamber. Hence, a simple evaluation based on different inlet pressures, showed that for 50% increase of operating pressure only swirl velocity is about 2.65% increased with respect to Skye's test condition 4.8 bar. Similarly, the same ineffective increasing of swirl velocity is seen at another axial location, also.

Effect of inlet pressure as one of the most important parameters in operating of a vortex tube can be analyzed from different point of views. Most of them were explained in the more details in the preceding sections. However, study of flow structure in the form of temperature distribution or path lines would be useful to realize of energy separation process. The obtained total temperature distribution contours are plotted in fig. 15. It shows peripheral flow to be warmer and core flow cooler relative to inlet temperature (294.2 K). Under operating condition of 4.8 bar, maximum hot gas temperature of 311.5 K and minimum cold gas temperature of 250.24 K is produced. For higher range of operating condition, 7.24 bar, maximum hot gas temperature 314.28 K and minimum cold exit 246.03 K can be achieved by this device, which is not very significant difference. These two pressure ranges imply to reasonable operating condition and conversely the condition that would be expected to take under the question the general idea of operation a vortex tube for any inlet pressure. As it is seen, the structure of total temperature contours for two models are almost the same, but there is only temperature difference in the lower and higher ranges of temperature levels. Thus, at the high inlet pressure 7.24 bar, the system wastes the input energy very considerable rather than the last one.

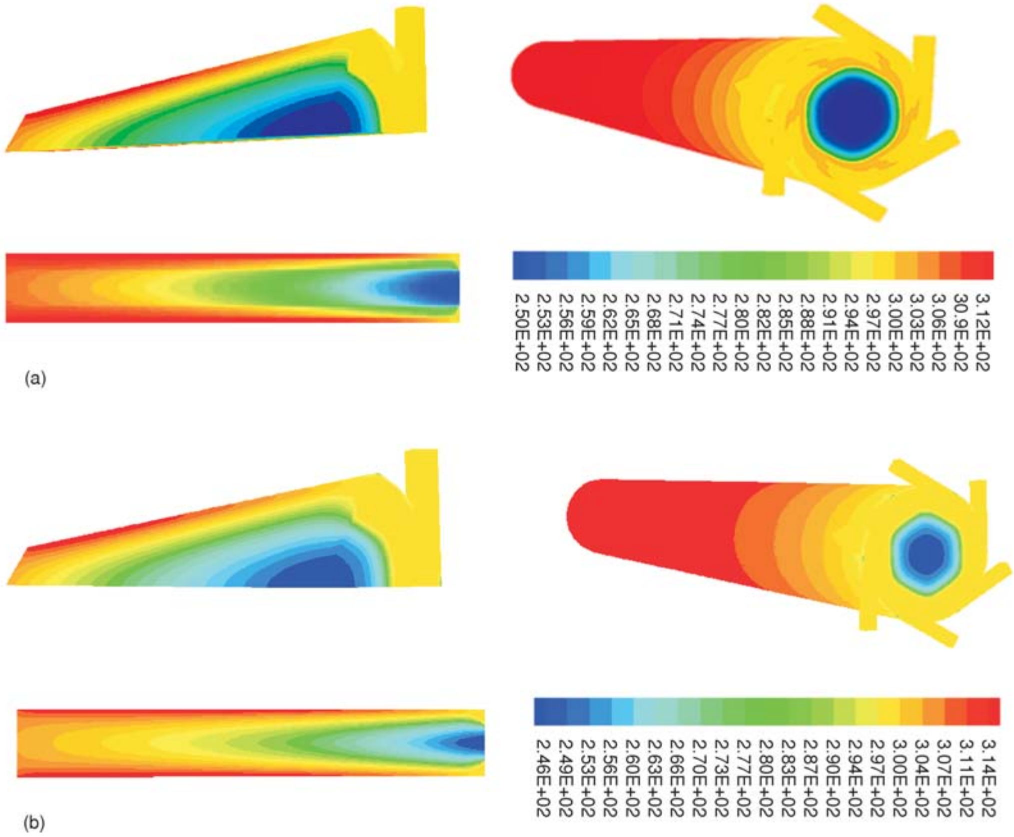

Figure 15. Temperature distribution in the vortex tube with (a) P_{in}= 4.8 bar, (b) P_{in}= 7.24 bar, α= 0.3 (for color image see journal web site**)**

Describing the flow patterns as path lines through vortex tube because of using different inlet pressures are depicted in fig. 16.

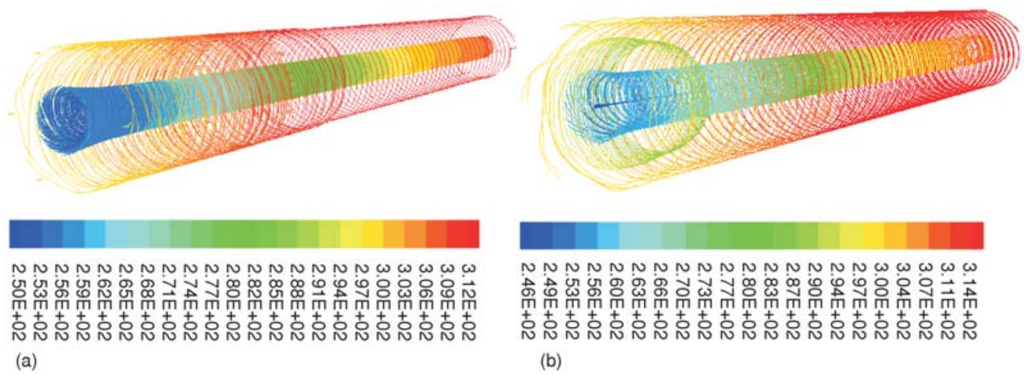

Figure 16. 3-D path lines colored by total temperature along the vortex tube with (a) P_{in}= 4.8 bar, (b) P_{in}= 4.8 bar, α= 0.3 (for color image see journal web site**)**

The formation of core and peripheral path lines can be clearly seen at the near of cold end and inner regions. The core vortex is disappeared after occurring of separation phenomenon. According to the numerical results of fig. 10, the axial location of separation point is very closer to hot exit end, and may be has difficulties in clarifying among the numerous path lines. Approaching to a properly symmetric rotational flow and intensively effective domain are seen in this figure for inlet pressure equal to 4.8 bar. Representation of path lines according to fig. 16(b) does not bring particular flow patterns, although the system benefits of more actuating energy.

Conclusions

In this research, a numerical investigation has been conducted to examine the performance of a vortex tube with respect to influence of different inlet pressures. The results of CFD models due to apply of various inlet pressures are derived and analyzed from different points of view. Hence, study of many criteria such as cold and hot exit temperature differences, probable occurring of shock wave in the vortex chamber in many cases, swirl velocity, and axial location of stagnation point were the main objects of investigation. The vast ranges of inlet pressure were chosen and utilized until the vortex tube performance shown the ineffective response to them. The Skye's acceptable experimental test condition, 4.8 bar, is confirmed with the obtained numerical results. Increasing of inlet pressure beyond this reference point makes an unbelievable flow behavior. Since, in spite of more energy consumption in those pressure ranges, some of analyzing criterion such as axial location of stagnation point becomes closer to Skye's lower pressure test condition. The purpose of present study to clarify of to be correspondent of any vortex tube with defined geometry, to a suitable inlet pressure is gotten based on the obtained numerical results; so that one can inferred that applying of inappropriate inlet pressure whether higher or lower will produce ineffective performance of device. In lower inlet pressure, it is evident that vortex tube system has insufficient input energy to provide the valuable swirl velocity. On the contrary, at the higher pressures because of geometrical restriction of vortex chamber there are not enough physical space or energy transferring opportunity for converging of input energy to desirable forms; that is injection to working fluid as angular momentum. The main reasons may be explored in occurring of strong shock waves in the vortex chamber just to exit ends of any nozzles. In this article it has been endeavored only to highlight the importance of inlet operating pressure, but there is not presented a general rule to attain the proper value of this parameter corresponds to both geometrical and physical conditions of working fluid. In this way, it would be proposed to conduct of libratory experimental tests or CFD numerical simulations procedures until a designed vortex tube can operate in reasonable degree of performance. It should be mentioned that economical features of cold exit gas producing by this machine are always preceded to other facts. In addition, the compatibility of presented numerical results with the available experimental data reveals the requirements of deeply investigation about this issue.

Nomenclature

D – diameter of vortex tube, [mm]
K – turbulence kinetic energy, [m^2s^{-2}]
L – length of vortex tube, [mm]
$\dot{m}_{in}$ – mass flow rate, [gs^{-1}]
R – radial distance measured from the centerline of tube, [mm]
P_{in} – inlet pressure, [bar]
S – the distance of nozzle entrance to core of high Mach number region
T – temperature, [K]
$\Delta T_{c,h}$ – temperature difference between cold and hot end, [K]
$\Delta T_{i,c}$ – temperature difference between inlet and cold end, [K]

$\Delta T_{i,h}$ – temperature difference between hot end and inlet, [K]
Z – axial length from nozzle cross-section, [mm]
$(Z/L)_w$ – axial location of maximum wall temperature
$(Z/L)_v$ – axial location of stagnation point

Greek symbols

α – cold mass fraction
ε – turbulence dissipation rate, [m^2s^{-3}]
μ – dynamic viscosity, [$kgm^{-1}s^{-1}$]
μ_t – turbulent viscosity, [$kgm^{-1}s^{-1}$]
ρ – density, [$kg\ m^{-3}$]
σ – stress, [Nm^{-2}]
τ – shear stress, [Nm^{-2}]
τ_{ij} – stress tensor components

References

[1] Ranque, G.J., Experiments on Expansion in a Vortex with Simultaneous Exhaust of Hot Air and Cold Air (in French), *J. Phys.Radium, 7* (1933), 4, pp. 112-114
[2] Hilsch, R., The Use of Expansion of Gases in Centrifugal Field as a Sooling Process (in German), *Rew Sci. Instrum., 1* (1946), pp. 208-214
[3] Elser, K., Hoch, M., The Performance of Various Gases and the Separation of Gas Mixtures into a Vortex Tube (in German), *Z. Naturf, 6a* (1951), pp. 25-31
[4] Martynovskii, V. S., Alekseev, V. P., Investigation of the Vortex Thermal Separation Effect for Gasses and Vapors (in Russian), *Soviet Physics, 1* (1957), pp. 2233-2243
[5] Takahama, H., Studies on Vortex Tube, *Bull. JSME, 8* (1965), 31, pp. 433-440
[6] Bruun, H. H., Experimental Investigation of the Energy Separation in Vortex Tubes, *Journal of Mechanic Engineering Science, 11* (1969), 4, pp. 567-582
[7] Skye, H. M., *et al*., Comparison of CFD Analysis to Empirical Data in a Commercial Vortex Tube, *Int. J. Refrig., 29* (2006), 1, pp. 71-80
[8] Fulton, C. D., Ranque's Tube, *J Refrig Eng., 58* (1950), 5, pp. 473-479
[9] Deissler, R. G., Perlmutter, M., Analysis of the Flow and Energy Separation in a Vortex Tube, *International Journal of Heat Mass Transfer, 1* (1960), 2-3, pp. 173-191
[10] Young, J., Mc Cutcheon, A. R. S., The Performance of Ranque-Hilsch Vortex Tube, *The Chemical Engineering*, *6* (1973), 1, pp. 522-528
[11] Ahlborn, B., *et al*., Limits of Temperature Separation in a Vortex Tube, *Journal of Physics D: Appl. Phys., 27* (1994), pp. 480-488
[12] Stephan, K., *et al*., An Investigation of Energy Separation in a Vortex Tube, *International Journal of Heat Transfer, 26* (1993), 3, pp. 341-348
[13] Stephan, K., *et al*., A Similarity Relation for Energy Separation in a Vortex Tub, *Int. J. of Heat Mass Transfer, 27* (1984), 6, pp. 911-920
[14] Dincer, K., *et al*., Experimental Investigation of the Effects of Length to Diameter Ratio and Nozzle Number on the Performance Counter Flow Ranque-Hilsch Vortex Tubes, *Heat Mass Transfer, 44* (2008), pp. 367-373
[15] Kirmaci, V., Optimization of Counter Flow Ranque-Hilsch Vortex Tube Performance Using Taguchi Method, *International Journal of Refrigeration, 32* (2009), 6, pp. 1487-1494
[16] Akhesmeh, S., *et al*., Numerical Study of the Temperature Separation in the Ranque-Hilsch Vortex Tube, *American Journal of Engineering and Applied Sciences, 1* (2008), 3, pp. 181-187
[17] Bramo, A. R., Pourmahmoud, N., A Numerical Study on the Effect of Length to Diameter Ratio and Stagnation Point on the Performance of Counter Flow Vortex Tube, *Aust. J. Basic & Appl. Sci., 4* (2010), 10, pp. 4943-4957
[18] Bramo, A. R., Pourmahmoud, N., CFD Simulation of Length to Diameter Ratio Effect on The Energy Separation in a Vortex Tube, *Thermal Science, 15* (2011), 3, pp. 833-848
[19] Pourmahmoud, N., Bramo, A.R., The Effect of L/D Ratio on the Temperature Separation in the Counter Flow Vortex Tube , *IJRRAS, 6* (2011), 1, pp. 60-68
[20] Pourmahmoud, N., *et al*., CFD Analysis of Helica Nozzles Effects on the Energy Separation in a Vortex Tube, *Thermal Science, 16* (2012), 1, pp. 151-166
[21] Aydin, O., Baki, M., An Experimental Study on the Design Parameters of a Counterflow Vortex Tube, *Energy, 31* (2006), 1, pp. 2763-2772

[22] Kirmaci, V., Uluer, O., An Experimental Investigation of the Cold Mass Fraction, Nozzle Number, and Inlet Pressure Effects on Performance of Counter Flow Vortex Tube, *Journal of Heat Transfer, 131* (2009), 081701-1

[23] Ameri, M., Behnia, B. The Study of Key Design Parameters Effects on the Vortex Tube Performance, *International Journal of Thermal Science, 18* (2009), 4, pp. 370-376

[24] Zhidkov, M. A., *et al*., Interrelation between the Separation and Thermodynamic Characteristics of Three-Flow Vortex Tubes, *Chemical and Petroleum Engineering, 37* (2001), 5-6, pp. 271-277

[25] Wu, Y.T. *et al*., Modification and Experimental Research on Vortex Tube, *International Journal of Refrigeration, 30* (2007), 1, pp. 1042-1049

Paper submitted: September 7, 2011
Paper revised: December 28, 2011
Paper accepted: February 8, 2012